Freely Available Datasets Able to Simulate the Snowmelt Runoff in Himalayan Basin with the Aid of Temperature Index Modelling

Asha Thapliyal[1] · Varun Khajuria[2] 🔟 · Praveen Kumar Thakur[2] · Sanjeev Kimothi[3] · Mahendra Pratap Singh Bisht[1] · Prakash Chauhan[2]

Abstract

The present study estimates snowmelt runoff in the Bhagirathi basin of the river Ganga using the snowmelt runoff model (SRM) with the freely available input datasets. A temperature index model WinSRM is used to calculate the discharge from simulated snowmelt runoff during 2010–2014. The variables of the model include precipitation, rainfall, air temperature, and snow cover area (SCA). Air temperature and precipitation are obtained from the MERRA-2 reanalysis and Indian Meteorological Department (IMD) gridded data, respectively, over the delineated zones of the basin. The SCA is estimated using the Moderate Resolution Imaging Spectroradiometer (MODIS) snow product: MOD10A2 data with an 8-day period or composite SCA of 500-m spatial resolution interpolated to a daily scale. Five-year simulation results show that the discharge maintains a high flow in monsoon with a mean value of 375.50 m^3/s. However, the model underestimates the average runoff volume by 7% in 2013 and overestimates it by 10% in 2010. The observed snow volume difference ($D_v\%$) is $-$ 10.32 and $+$ 4.36 for the years 2010 and 2012, respectively. Measured and simulated discharge rates are found to be in agreement with correlation coefficients in the range of 0.81–0.84 during the 2010–2014 period. Simulated discharge rates showed strong variability with typically highest values from mid-June to August (e.g. 3400.31 m^3/s in 2013). The model also showed some additional peaks in September and June as seen in measurements during 2010, 2013, and 2014. Average runoff rates during the monsoon season (June–August) were estimated to be in the range of 478.69–689.23 m^3/s during the study period. This study reveals the contiguity of the model results as compared with the real-time observations and indicates potential for improvement with the usage of satellite-derived inputs within the deviation limits. The findings from the study have implications for better monitoring of glacier health, snowmelt runoff, and natural resource management in the Himalayas, where meteorological and hydrological observations are limited.

Keywords Snowmelt · Runoff · Degree-day factor · SRM model

✉ Varun Khajuria
varunkhajuria10@gmail.com

Asha Thapliyal
ashath08@gmail.com

Praveen Kumar Thakur
praveen@iirs.gov.in

Sanjeev Kimothi
drskimothi@gmail.com

Mahendra Pratap Singh Bisht
mpbisht@gmail.com

Prakash Chauhan
prakash@iirs.gov.in

[1] Uttarakhand Space Application Centre, Upper Aamwala, Nalapani, Dehradun, Uttarakhand 248001, India

[2] Indian Institute of Remote Sensing, ISRO, Dehradun, Uttarakhand 248001, India

[3] Graphic Era Deemed to be University, Bell Road Clement Town, Dehradun, Uttarakhand 248002, India

🊑 Springer

Introduction

Rapid urbanization and an increase in population in the Himalayan region have enhanced freshwater consumption significantly, and therefore accurate predictions of melt-derived stream flow using hydrological models are of paramount importance. The Himalayan region is a fragile ecosystem with steep topography where natural calamities such as landslides and flash floods are frequently observed (Singh & Baym, 2006). Himalayan glaciers have a substantial impact on high-terrain hydrology. In addition, they support ecological life in South and Central Asia by providing water resources (Mankin et al., 2015; Shrestha et al., 2015). Snowmelt runoff is the primary source of freshwater for the large population located in the high hilly region of Uttarakhand. Efficient water resource management is therefore needed to address the issues such as fresh water supply, flood forecasting, and climate change impacts in the Himalayan region. The local weather systems and mountain-induced dynamic and thermodynamic processes affect the precipitation pattern, cloudiness, etc., and contribute to snowfall and snowmelt in the Himalayas (Khadka et al., 2014). Physical properties along with the local meteorological conditions are therefore important to snowmelt at the land–atmosphere interface. Snowmelt has a linear relationship with air temperature, which influences the snow cover and precipitation in the atmosphere (Qin et al., 2006).

Past SCA studies show that December and June months witnessed significant changes (Joshi et al., 2014; Singh et al., 2019). December experienced a declining trend in snow cover between 3000 and 6000 m a.s.l. covering 88% of the basin area, whereas June showed an increasing trend between 4500 and 6000 m (a.s.l.). September and October experienced the highest inter-annual snow cover variability. The maximum snow cover month of February and minimum snow cover month of August experienced the least variability (Joshi et al., 2014; Singh et al., 2019). SCA was found to increase across all the elevation zones in winter; the rate of increase was particularly high in the lower elevation zones as compared with higher and middle elevation zones (Joshi et al., 2014; Singh et al., 2019). Additionally, the satellite datasets (i.e. MODIS, ALOS PALSAR) are analysed to understand the snow cover extent and snowmelt in the Bhagirathi basin of the Himalayan region. These parameters are sparsely measured in high-altitude regions; nevertheless, they can be obtained from satellite retrievals to drive runoff models (Rango, 1985; Wulf et al., 2016). Snow characteristics have also been obtained using inversion techniques from multispectral satellite data in various studies (Dozier, 1989; Fily et al., 1997; Hall et al., 2001; Jain et al., 2010a, 2010b;

Kokhanovsky et al., 2011; Painter et al., 2003; Sood et al., 2021).

The Uttarakhand Himalaya is a reservoir of glaciers and feeds two rivers, i.e. the Alaknanda and Bhagirathi. Hydrologically, these are the major headwater tributaries of the holy river Ganges in the Indian Himalayas, mainly due to their area, several glaciers, and seasonal snow. The headwaters of the Bhagirathi are formed at Gaumukh at the foot of the Gangotri glacier and Khatling glacier in the Garhwal Himalaya. The decadal variability of these glaciers has been studied using LISS-III/IV, AWIFS, ASTER, and CARONA, etc., to quantify the temporal change in the glacier area, glacier length, elevation, surface velocity, and direction of flow (Bhambri et al., 2011; Jain et al., 2010a, 2010b; Kumar et al., 2021; Kokhanovsky et al., 2011). The factors contributing to the glaciation of an area include the height of the ridges, the orientation of slopes, temperature, and precipitation in the area (Narama et al., 2010).

Snowmelt and melt flux modelling using an energy balance approach and process-based modelling involves meteorological datasets such as cloud cover, cloud temperature, incoming and outgoing solar radiation, and wind and dew-point temperature (Todd Walter et al., 2005; Anderson, 1973; Ångström, 1933). Snowmelt directly impacts stream flow and affects the freshwater supply, irrigation, and hydropower potential of the region. Hence, consistent glacial runoff datasets are essential to investigating water allocation in the Himalayan region. Snowmelt modelling has generally been conducted using heat balance equations as in energy balance models or by using empirical relations between melt rate and air temperature, i.e. the temperature index model (Fierz et al., 2003; Singh et al., 2010). Temperature index models have been more common due to computational simplicity. Numerous studies (Abudu et al., 2016; Aggarwal et al., 2014; Azam et al., 2019; Jain et al., 2009; Khajuria et al., 2022; Prasad & Roy, 2005; Singh et al., 2021; Bhadra et al., 2015; Zhang et al., 2006) have applied temperature index-based modelling following its applications to flood forecasting and hydrological modelling. The temperature index method is suggested to be especially useful over complex terrains and when meteorological observations are sparse (Hock, 2003). Variability in melt runoff in the Himalayan region has remained unclear due to a lack of ground-based datasets. Therefore, the degree-day approach has been used more widely for snowmelt modelling (Liu et al., 2006, 2007; Li & Wang, 2008; Li & Williams, 2008; Ma & Cheng, 2003; Martinec et al., 1994; Quick & Pipes, 1995; Wang et al., 2009; Pangali Sharma et al., 2020).

The SRM has been applied successfully in the Himalayan region for runoff estimation (Aggarwal et al., 2014;

Azam et al., 2019; Jain et al., 2010a, 2010b; Narama & MacClume, 2010; Pangali Sharma et al., 2020; Singh et al., 2021; Tayal Senzeba et al., 2015). The model inputs include zonal SCA and meteorological variables such as daily precipitation and air temperature. Incorporation of local topographical parameters, e.g. terrain slope, aspect, elevation, etc., and varying meteorological conditions improves the accuracy of snowmelt estimations (Bormann et al., 2014; Marsh et al., 2012; Sood et al., 2021).

Consequently, the present study is aimed at monitoring the temporal and spatial distribution of the snow cover area (SCA) and estimating the snowmelt runoff for the Bhagirathi basin. In this study, we have used the temperature index-based snowmelt model due to its simplicity and reliance on the degree-day approach (Martinec et al., 2008).

Study Area

Bhagirathi, a sub-basin of the Ganga River, emerges from Central Himalaya and lies between longitude (78°9′15″ E–79°24′55″ E) and latitude (30°20′20″ N–31°27′30″ N) in the trans-Himalayan region. A total of 494 glaciers have been identified in the basin covering a total area of 721.64 km^2 (RGI Consortium, 2017). The snout of the Gangotri glacier is the source of the river Bhagirathi, and at Devprayag, it meets with Alaknanda to form the River Ganges. The total catchment area of the river Bhagirathi is 7295 km^2 delineated using the Tehri dam as the outlet and lies in the Uttarkashi and Tehri Garhwal districts of Uttarakhand. The Bhagirathi sub-basin rises from 667 m to an elevation of 7045 m with a mean elevation of 3856 m. The catchment receives most of the rainfall during the southwest monsoon. Annual rainfall ranges from 1016 to 2630 mm. Most of its snow is the principal source of water for the major tributaries of the river Ganga. Garhwal Himalayan glaciers are fed by summer monsoon and winter snow regimes (Thayyen & Gergan, 2010). However, maximum snowfall occurs from December to March, mostly due to western disturbances (Dobhal et al., 2008). The study area is distributed into twelve different elevation zones as shown ranging from (667–1000 m), (1000–1500 m), (1500–2000 m), (2000–2500 m), (2500–3000 m), (3000–3500 m), (3500–4000 m), (4000–4500 m), (4500–5000 m), (5000–5500 m), (5500–6000 m), and (> 6000 m) using ALOS PALSAR DEM as shown in Fig. 1. The catchments are subdivided into the watersheds of Bhagirathi, Bhilangana, and the river Asi Ganga.

Materials and Methods

Regions under different elevation zones are extracted using GIS techniques for the Bhagirathi basin. To derive the hypsometric curve, the area–altitude distribution is generated for the basin. The ALOS PALSAR—Radiometric Terrain Corrected DEM with pixel size 12.5 m for high resolution (RT1) is used to create the elevation bands or zones for the selected river basins of the study area. The high-resolution sensing ability of ALOS PALSAR DEM provides more ground feature details for the highly rugged terrain in comparison with the SRTM DEM (Sharma et al., 2010; Tulu, 2005). Basin characteristics, e.g. mean elevation, aspect is derived from the ALOS PALSAR DEM.

The GIS tool is used to subdivide the basin boundary into different elevation zones, and the zonal statistics tool is used to calculate the statistics of each zone (Table 1). The zonal mean hypsometric elevation is calculated from the curve plotted between the cumulative zone area and the elevation range (Fig. 2). The basin characteristics (such as the individual zone area and its mean hypsometric elevations, percentage aspect area, and average elevation aspect zone-wise) are used as input to the SRM model. The hypsometric curves are then used to calculate the mean elevations of the river basins and their respective altitudinal zones. ALOS PALSAR DEM is used to calculate the zonal areas and the area distribution (hypsometry) curve for each zone.

The maximum area of the basin belongs to the eleventh elevation zone (5000–5500 m) and occupies 15.4% of the total area (1127.25 km^2), whereas only about 1.98% of the area is in the twelfth elevation zone (> 6000 m). The hypsometric zone elevation of various delineated zones is summarized in Table 1. The hypsometric mean zone elevation varies from 853 to 6218 m for zone ids 1–12, respectively.

The aspect area of each zone shown in the table was also derived for four directions, i.e. north-east, south-east, north-west, and south-west, to consider the zone-wise percentage aspect area of the basin and to consider the topographic features of the basin; it also improves the accuracy of the simulation. The effects of the sun's rays on the north, south, east, and west on-air temperatures can be significant. According to Kang (2005), snow albedo varies depending on the snow surface properties and melting processes. Given the importance of topography, incorporating topographic parameters such as aspect and slope into the estimation of a number of degree days in the temperature index model could increase the SRM model's accuracy in mountain watersheds (Table 2).
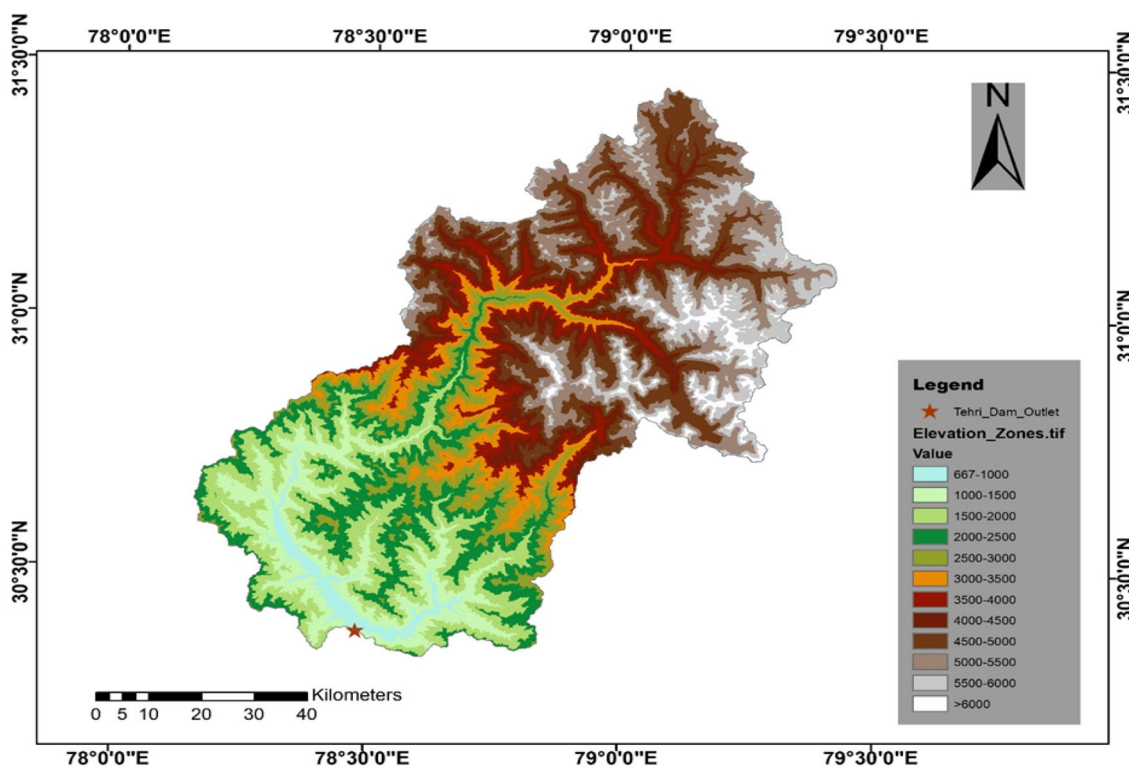
Fig. 1 Study area map showing different elevations zones

Table 1 Area of each elevation zone with hypsometric mean elevation

Zone	Elevation in (m)	Area in Sq.km	Cumulative area	Hypsometric mean elev.(m)
1	667–1000	146.13	146.13	853
2	1000–1500	597.85	743.98	1287
3	1500–2000	912.15	1656.13	1754
4	2000–2500	784.20	2440.33	2232
5	2500–3000	505.69	2946.02	2737
6	3000–3500	453.05	3399.07	3248
7	3500–4000	448.43	3847.5	3755
8	4000–4500	590.52	4438.02	4270
9	4500–5000	992.91	5430.93	4769
10	5000–5500	1127.25	6558.18	5243
11	5500–6000	591.95	7150.13	5704
12	> 6000	145.11	7295.24	6218

Hydro-Meteorological Datasets

The hydro-meteorological data comprise daily air temperatures and daily rainfall measured at different stations in a basin. The model uses a zonal-based approach derived from a digital elevation model (DEM) and estimates precipitation, temperature, and snow cover area for each zone. Using these elevation zones, the mean of each elevation zone is calculated from hypsometric curves, which are used to extrapolate the base station temperatures to different elevation zones and to calculate the degree-day factor and

snowmelt runoff coefficient (Cs), rainfall–runoff coefficient (Cr) in each elevation zone.

A high spatial resolution (0.25° × 0.25°) daily gridded rainfall dataset of IMD shown in Fig. 3 was used in the basin, and the rainfall was then converted to zonal rainfall; the IMD data show good results over the Himalayan basins as compared with other datasets.

Furthermore, the spatial precipitation conveyance like heavy rainfall regions in the orographic areas of the west coast and over the upper east, low precipitation in the leeward side of the Western Ghats, and so forth were more
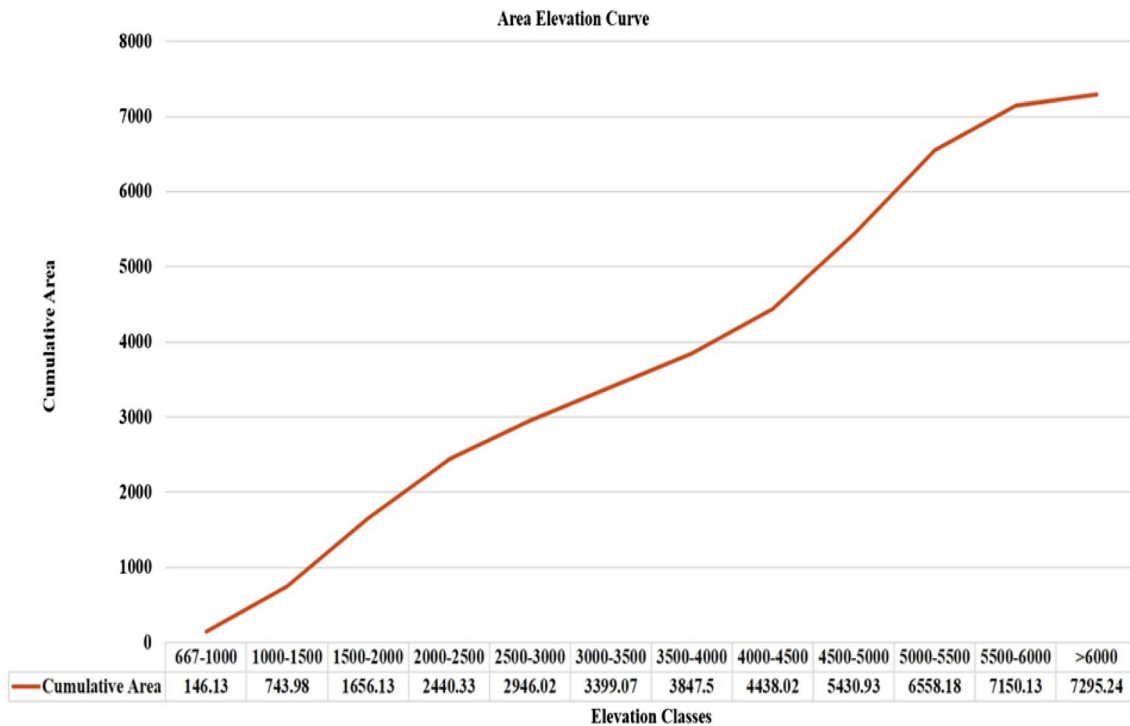
Fig. 2 Area elevation curve

practical and better introduced in IMD because of its higher spatial goal and to the higher thickness of precipitation stations utilized for its development (Pai et al., 2014). The daily temperature used and measured at a few stations in the Bhagirathi basin was then extrapolated spatially by applying the lapse rate correction across the entire basin to account for spatial variability in the proposed snowmelt runoff model. The extrapolated temperature is shown in Fig. 4. For this purpose, spatial interpolation techniques such as inverse distance squared (IDS) with multiple regression approaches are applied, in which the range of input parameters such as spatial distance, elevations, and temperatures has been used.

Due to the scarcity of the hydro-meteorological stations in the higher Himalayan region, the rainfall data available from IMD and temperature data from MERRA-2 reanalysis product at 2 m are extended to higher elevation zones based on the relationship between rainfall, temperature gradient, and elevation. After the delineation of the study area boundary, the snow cover fraction was generated by interpolating weekly to daily snow cover data using regression techniques. Division of the catchment in elevation zones provides better estimates of the snow cover area as depicted in Fig. 5.

This method will help in accurately determining the melt runoff contribution from each zone. The SCA is derived using MODIS satellite data 8-day products (MOD10A2) at 500 m spatial resolution which was then interpolated at the daily scale, and then, the daily value of conventional depletion curves was used for simulation of SRM over the delineated zones ranging from 667 to 7045 m altitude. The boundary conditions for elevation, spatial distance, and expected temperature of the unknown location are within the input station regimes and location temperature, respectively. In situ melt runoff estimation is challenging due to the limited accessibility of high-altitude terrains and the lack of direct measurements of input parameters to drive model simulations (Pangali Sharma et al., 2020). Therefore, hydro-meteorological datasets (e.g. air temperature and precipitation) have been obtained from the IMD (https://www.imdpune.gov.in/), and air max, min, and mean temperature from NASA prediction of worldwide energy resources project which provides solar and meteorological datasets (https://power.larc.nasa.gov/). These datasets are obtained for different elevation zones during the 2010–2014 period. The daily temperature and precipitation for each zonal hypsometric elevation are derived by extrapolating the average dataset obtained at the delineated point base stations. Figure 4 shows the average temperature variation zonal-wise in the basin with a maximum average temperature of 18.65 °C and a minimum average temperature of − 10.35 °C. The catchment receives moderate-to-heavy rainfall during the monsoon, whereas during winter, it receives moderate snowfall at higher altitudes and heavy rainfall at lower altitudes. The river Bhagirathi runoff during monsoon is stronger due to

Table 2 Aspect area of each zone

Zone	Aspect	Area (Sq. km)	% Area
1	North-east	51.179	35.02306
1	South-east	30.136	20.62246
1	North-west	37.446	25.62479
1	South-west	27.370	18.72969
2	North-east	155.975	26.08932
2	South-east	141.649	23.69307
2	North-west	167.851	28.07577
2	South-west	132.377	22.14218
3	North-east	221.222	24.25281
3	South-east	224.338	24.59442
3	North-west	252.786	27.71321
3	South-west	213.810	23.44022
4	North-east	186.906	23.83397
4	South-east	194.111	24.75274
4	North-west	213.562	27.2331
4	South-west	189.630	24.18133
5	North-east	117.503	23.23617
5	South-east	128.851	25.48023
5	North-west	130.187	25.74443
5	South-west	129.151	25.53956
6	North-east	102.878	22.70787
6	South-east	117.660	25.97064
6	North-west	116.054	25.61616
6	South-west	116.467	25.70732
7	North-east	110.923	24.73586
7	South-east	109.155	24.34159
7	North-west	121.600	27.11683
7	South-west	106.757	23.80684
8	North-east	154.953	26.24009
8	South-east	136.643	23.13944
8	North-west	155.776	26.37946
8	South-west	143.151	24.24152
9	North-east	269.919	27.18464
9	South-east	235.144	23.68231
9	North-west	246.367	24.81262
9	South-west	241.488	24.32124
10	North-east	294.645	26.13839
10	South-east	288.222	25.5686
10	North-west	287.479	25.50268
10	South-west	256.905	22.79042
11	North-east	146.665	24.77659
11	South-east	148.662	25.11395
11	North-west	155.075	26.19731
11	South-west	141.555	23.91334
12	North-east	34.775	23.96458
12	South-east	33.557	23.12515
12	North-west	35.783	24.65929
12	South-west	40.998	28.25284

heavy and prolonged rainfall. The runoff from March to June predominantly depends on the snowmelt. A zonal-wise (Fig. 6) analysis is conducted for the dispersion of seasonal zonal rainfall over the Bhagirathi basin during the 2010–2014 period. The zonal-wise rainfall over the basin particularly varies between 2 and 18 cm. The observed discharge data are available with us at the defined outlet point in the model, i.e. Tehri dam, and then, the model is calibrated for three years using the critical parameters of the model after successfully calibrating the model and then validated using the same parameters for two years of span.

Satellite Datasets

The Moderate Resolution Imaging Spectroradiometer (MODIS)/Terra snow cover product comprises the snow cover extent data and has a resolution of 500 m covering the Bhagirathi basin. The Terra (EOS AM) satellite overpasses the equator in the morning and provides high radiometric sensitivity measurements in 0.4–14.4 μm wavelengths (Hall et al., 1995). MOD10A2 data products available from the GSFC website (http://modis.gsfc.nasa.gov) have been used to generate snow cover input for SRM. Daily values for snow cover were obtained from 8-day composite snow cover using the interpolation technique. The snow cover in the basin is also shown in Fig. 7 for all the months; the maximum snow cover area was observed in the months of December, January, and February, and the minimum snow cover was observed in the month of July, August, and September. The maximum and minimum snow cover areas vary approximately from 70 to 20% of the total basin area. In the current study, the SCA has been utilized for various elevation zones as the main input variable of the model. For this reason, SCA maps have been prepared for each day over the simulation period. The SCA was then plotted against the time to develop the conventional depletion curves for the different elevation bands in the catchment on a daily time step. The snow cover depletion curves differ from year to year; it has been prepared independently for each year. To simulate the observed runoff with the computed one on daily basis, data and day-to-day SCA for each band were utilized as input parameters in the model.

Snow Runoff Model (SRM)

The deterministic model 'SRM', based on a degree-day approach, is used to simulate and forecast the runoff from snowmelt in a basin (Martinec et al., 2008). This is one of the most extensively used runoff models due to its computational simplicity and lesser dependence on meteorological datasets. It is based on an empirical relation between melting and air temperature and relies on variables
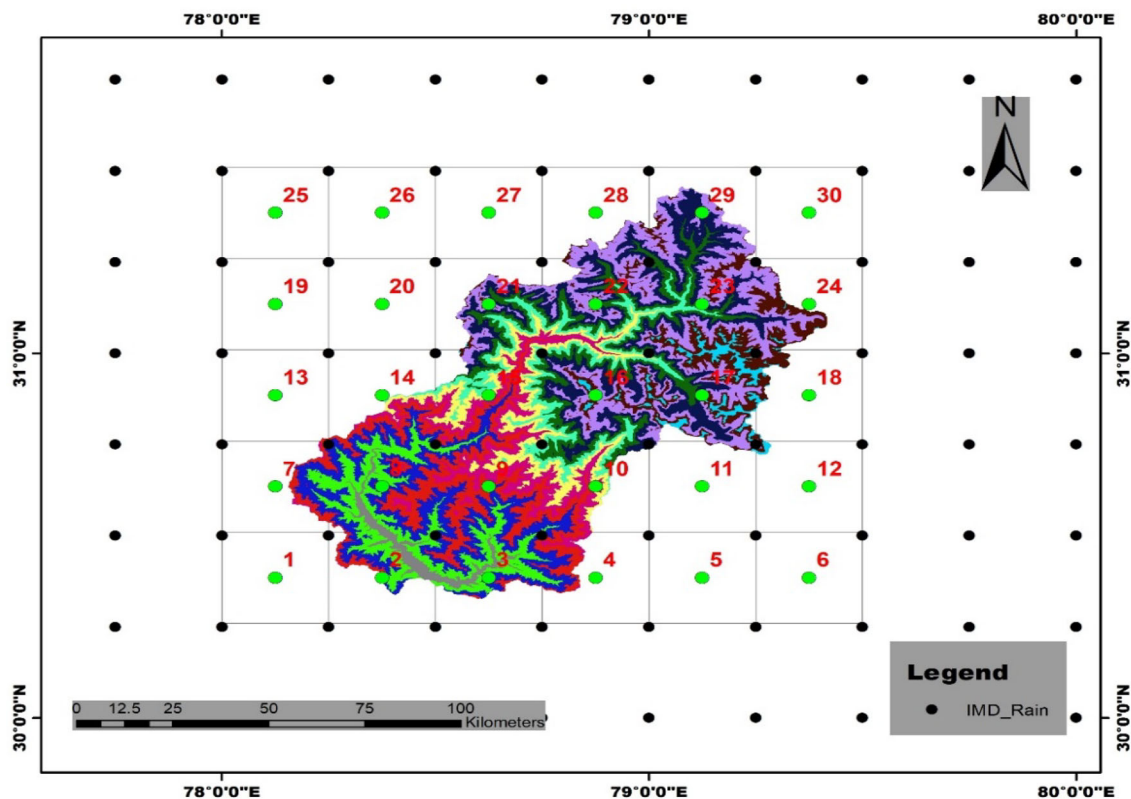
Fig. 3 Zonal rainfall conversion

such as precipitation, maximum and minimum or average temperature, and changes in SCA (Martinec et al., 2008). In addition to the input variables, a number of basin characteristics such as basin area, zone area, and the hypsometric (area elevation) curve are also needed. SRM has been applied to simulate stream flow from time series precipitation datasets for the period of 2003–2009 in the Buha watershed region (Zhang et al., 2014). WinSRM-1.12 has been used to simulate the snow runoff due to its applicability over diverse terrains (over the Himalayan region) and relatively minimal requirements for essential data inputs (Aggarwal et al., 2014; Azam et al., 2019; Jain et al., 2010a, 2010b; Kulshrestha et al., 2018; Pangali Sharma et al., 2020; Singh et al., 2021; Thakur, 2014).

The degree-day factor (DDF) is the coefficient of proportionality $f = \left(\frac{a}{\varphi}\right)$ between surface ablation 'a' and the positive degree-day sum 'φ' over the period. It is also known as the melt coefficient and signifies the amount of melt that occurs as a positive degree day. The DDF was averaged and found to be 0.30–0.65 cm °C^{-1}d^{-1} for April to August during the 2010–2014 period. The DDF value is kept low at the beginning of the melting season when the glacier is covered with seasonal snow and increases up to the end of the season. The major SRM parameters for model calibration include critical temperature T_{CRIT}; DDF;

temperature lapse rate γ; runoff coefficient including that from rain (Cr); and runoff coefficient from snowmelt (Cs); rainfall contributing area (RCA); recession coefficient (K) of x and y parameters; lag time (L); X and Y coefficients are part of the recession coefficient (K); the ratio of the snow-covered area (SCA) to the total area (S); sequence of days (n) (Martinec et al., 2008).

Kulshrestha et al., (2018) investigated degree-day snowmelt runoff using a temporal variation of near-surface lapse rate (0.65–0.75) °C per 100 m and recommended the use of monthly value instead of a yearly value in the temperature index-based models for Himalayan basins. The lapse rate varies from 0.30 to 0.65 for all the zones of the basin. Other variables such as Cs and Cr vary from 0.10 to 0.8, the rainfall contributing area (RCA) is 0 to 1 (0 for October to March and 1 for April to September), $X_{coefficient}$ varies from 0.96 to 1.05, and $Y_{coefficient}$ is kept to be 0.088 for all the basin zones for all studied years. A description of the various parameters used in the model is given in Table 3. Snow runoff estimation and evaluation of the model are carried out with two statistical indices, i.e. coefficient of determination (R^2) and the volume difference percentage (Dv%). Daily average snowmelt discharge Q is calculated by DDF combined with the positive temperature approach, and a detailed description of the variables and parameters used is given by Martinec et al., (2008). The
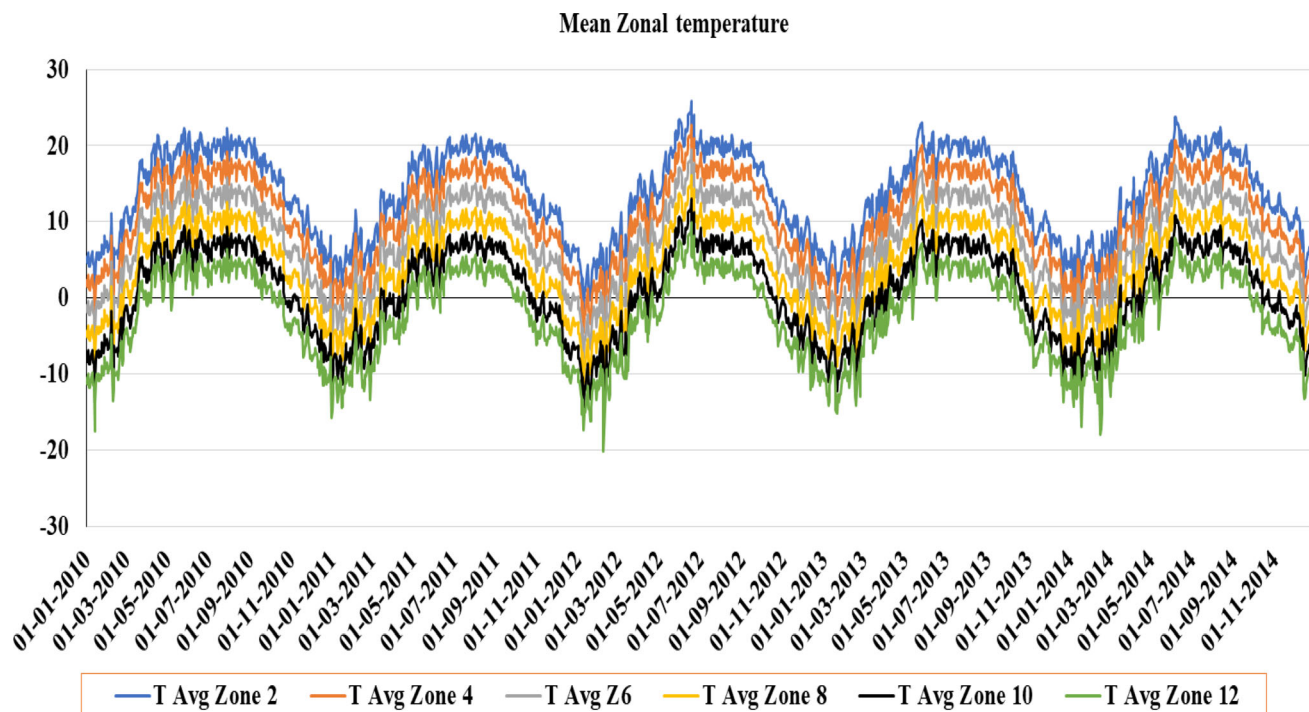
Mean Zonal temperature

Fig. 4 Zonal temperature

daily water produced from the snowmelt and rainfall is superimposed on the calculated recession flow and transformed into daily discharge from the catchment according to the following Eq. (1):

$$Q_{n+1} = C_{Sn}a_n(T_n + \Delta T_n)S_n$$
$$+ C_{Rn}P_n \frac{A*10,000}{86,400}(1 - K_{n+1}) + Q_n K_{n+1} \quad (1)$$

The daily temperatures in various elevation zones have been calculated from the base station using Eq. (2) (Martinec et al., 2008), and the temperature lapse rate is given by Eq. (3):

$$T' = (T - \Delta T) \quad (2)$$

and

$$\Delta T = \gamma \cdot (h_\alpha - \overline{h}) \cdot \frac{1}{100} \quad (3)$$

The recession coefficient is determined by:

$$K_{n+1} = x \cdot Q_n^y \quad (4)$$

where ΔT is an adjustment by temperature lapse rate when extrapolating the temperature from the base station to the average hypsometric elevation of the basin or zone. γ temperature lapse rate (0.65 °C per 100 m), h_α altitude of the temperature station (m), $\overline{h}$ hypsometric mean elevation of a zone (m), T' daily mean temperature in different zones, and T daily mean temperature at the base station. The widely used snowmelt computation approach is easy to

extrapolate or interpolate on climate and spatial timescales. The approach is based on an empirical relation that relies on meteorological variables and requires calibration to adjust the suitable inputs as per the environment of the basin.

Calibration

The snow runoff model (SRM) parameters are sensitive, especially for the Himalayan region, which has high terrains and less predictable meteorological variations. The SRM parameters along with runoff coefficients (Cs and Cr) are widely used parameters in model calibration due to their spatial and temporal characteristics. Calibration of SRM is carried out for different model parameters through trial-and-error comparing simulated and measured hydrographs flow. The model is calibrated over various delineated zones for the hydrological period (April to August) during 2010–2014. The various input parameters with their used ranges in the calibration are shown in Table 3. Remotely sensed snow cover, extrapolated temperature, and precipitation are combined to estimate the snowmelt runoff dynamics. The optimized parameters are used for a simulation with the assimilation of the different parameters and coefficients. The model outcomes are validated with observed point source discharge data, considering climatic and hydrological data besides the contribution of major tributaries of the river Bhagirathi.
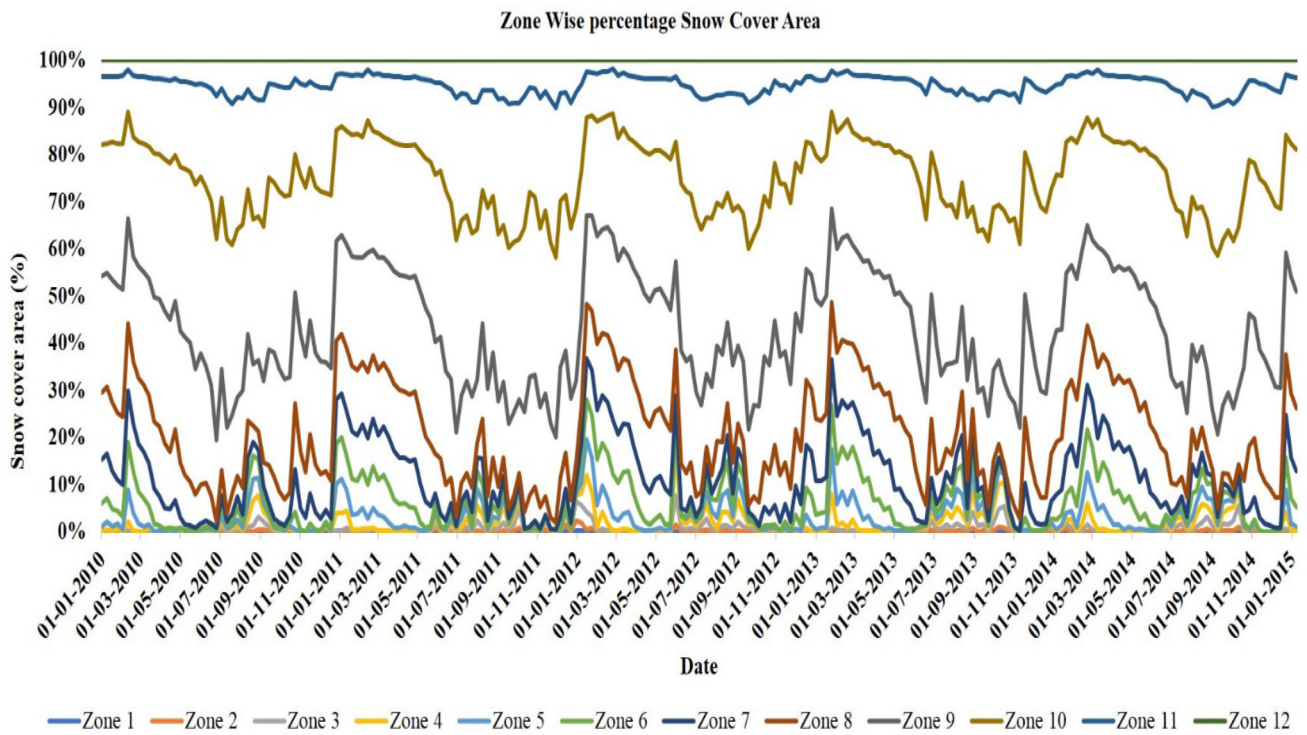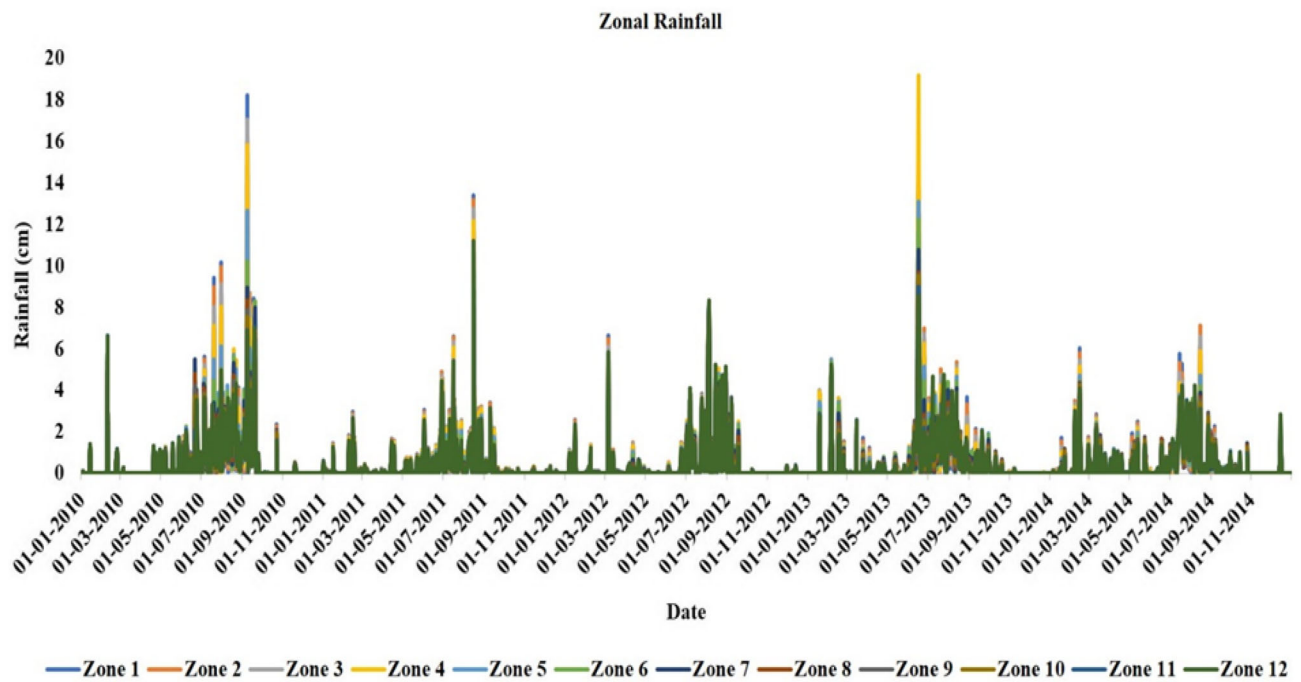
Fig. 5 Zone-wise snow cover area
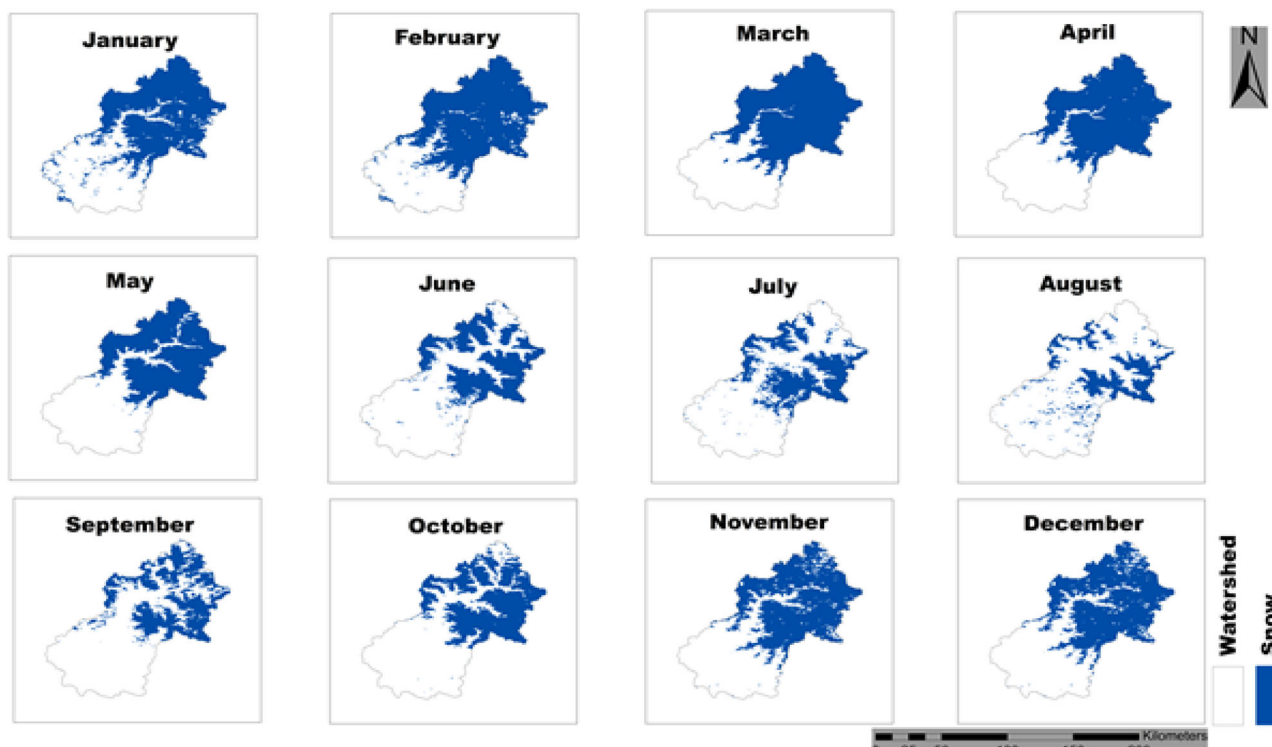

Fig. 6 Zonal rainfall

Fig. 7 Mean monthly snow cover area for all years

In this research, the calibration period of the model is from 2010 to 2012, and the validation period is from 2013 to 2014. Calibration of the SRM model is manually done by varying the model parameters within the permissible range and (by comparing the simulated and measured hydrographs of flow with the trial-and-error techniques).

For model calibration, the initial SRM parametric values, including γ, Tcrit, Cs, Cr, and RCA, are tested with multiple variables and parameter configurations by trial and error to understand the relationship between the inputs and their simulated hydrographs (Martinec and Rango 1986). These parameters are extracted from the studies conducted previously (Kulshrestha et al., 2018) on the - Himalayan regions. Lapse variation was noted in the basin; the higher value of lapse was found in April, May, and June, and a lower value was noted in July and August.

These parameters are tested and configured, and their simulated hydrograph relationships are obtained. A parameter adjustment technique was used in a zone-wise approach at a daily time step. The model is iteratively calibrated with the achievable range of NSE values (i.e. equal to or more than 0.65) for obtaining the optimum of local parameters (Kult et al., 2014). The permissible range of various parameters after adjustment in the calibration mode is monitored in the simulation. The runoff model was calibrated for different study periods and analysed the performance of two well-established accuracy criteria, R^2

and $D_v\%$ range of discharge (m^3/s) during the ablation period. The air temperature and rainfall data obtained from the MEERA-2 and IMD are used which is at spatial resolutions of 0.25° × 0.25° and 0.5° × 0.625°, respectively.

Results and Discussion

Hydrological and meteorological conditions in the high-terrain region are closely associated with the topographical variation of the region. The observed meteorological point source data obtained from IMD and MERRA-2 are matched with selected hypsometric mean elevation for various zones. An area with altitudinal variation (Fig. 2) is computed and indicates the middle zone 5–9 covers 40.99% of the area of the basin; it also shows at most 33.45% of the area falls within lower zones 1–4. About 25.55% of the basin area is occupied by higher elevation zones 10–12.

Plots for precipitation data distribution for 2010–2014 shown in Fig. 2 reveal that the released water quantity from glacial areas depends directly on the snow extent; therefore, it is introduced as a state variable in this hydrological model. The precipitation datasets exhibit small dispersion during the winter months of the studied hydrological years as shown in (Fig. 6). Large dispersion and clustering are observed during July and August. As seen from (Fig. 6) extreme or higher rainfall events are frequent from July–

Table 3 Calibrated parameters

Parameters	Range	Description
Lapse rate (°C/100 m)	0.4–0.69	Lapse rate was found to be low during the months of July and August and high in April, May, and June
Critical temperature (°C)	0 °C	Constant for all zones
Time lag	18 h	Constant for whole basin
Runoff coefficient for snow, C_s	0.15- 0.80	High during monsoon season and low during rest of months
Runoff coefficient for rain, C_r	0.20- 0.80	High during monsoon season and low during rest of months
Degree-day factor (cm $°C^{-1}$ d^{-1})	0.30–0.55	April to November (0.30) and when melt occurs (0.55)
Rainfall contribution area, RCA	0–1	Varied month wise and zonewise
X_{coeff}	1.0289	Constant for whole basin
Y_{coeff}	0.088	Constant for whole basin

September over the five years of observations during 2010–2014. The bimodal distribution exhibits higher amounts of rainfall in monsoon months from June to September accounting for the maximum rainfall during the months of July and August in each year. The average precipitation over the basin, particularly at the delineated points, varies between 2 and 30 mm.

The plots of average extrapolated zonal temperature in Fig. 4 show that the average temperature in the basin varies from 18.35 to − 10.35 °C. The uncertainty in the temperature and rapid fluctuations in the precipitation affects the SCA, and therefore, the snow depletion trends vary as can be seen in Fig. 5 (Joshi et al., 2015). The Earth's radiation budget and water availability are directly influenced by the presence of the SCA, which makes it a key parameter for studies in hydrology, meteorology, and climatology. Hence, the snow cover fraction is determined by interpolating MODIS 8-day data to daily snow cover, and then, the depletion curves are obtained. The spatial distribution of the SCA (shown in Fig. 7) for different months during 2010–2014 indicates that the depletion of snow-covered areas varies as the temperature fluctuates. SCA is observed to be lesser during rainy conditions of summer in the lower zones and higher in the winter.

The maximum accumulation is found during the accumulation period, i.e. December to February months due to a decrease in temperature and high snowfall over the basin. Similarly, in the monsoon season (July–September), the SCA is minimum and optimum during October, November, and December and such trends are seen in the five years of datasets with few uncertainties. The maximum and minimum snow cover areas vary approximately from 70 to 20% of the total basin area. Because of the large size of the Gangotri glacier, the river Bhagirathi is a full-fledged river even as it emerges from the subglacial tunnels at the glacier terminus of the Gaumukh. The daily zonal SCA fraction trend for the Bhagirathi River basin is shown in Fig. 5. The snow cover is seen to increase during the winter to the autumn season and decrease during the summer to monsoon. The study investigates the impact of effects of extrapolated temperature and SCA (snow-covered area) fraction patterns on diurnal flow (Fig. 8).

The comparison between simulated and observed discharge for five hydrological years during 2010–2014 is plotted in Fig. 9. It is found that the simulated and measured discharge values are strongly correlated in the April–May months and fluctuated during the monsoon months, i.e. July–August. This is due to the lower variation in temperature and precipitation. From the hydrograph in Fig. 8 for the year 2010, the simulated discharge rate varies from 28.23 to 1703 m³/s and increases gradually with temperature attaining a maximum peak in the month of August and September. During the hydrological year 2011, the simulated discharge rate varies from 32.10 to 2200.41 m³/s and a high peak was observed during mid of August month. In the hydrological years 2013 and 2014, the lowest discharge rates are simulated to be 25.69 and 32.34 m³/s, respectively, and the highest values are 3400.31 and 1236.94 m³/s, respectively. The model was also able to predict the peak during the year 2013, in which the THDC saved the downstream area through reservoir operations. The volume difference percentage is 3.55, 4.36, and 7.38 for the years 2011, 2012, and 2013, respectively, whereas overestimation of − 10.32 and − 12.45 is found during 2010 and 2014, respectively. Underestimation of discharge for the June peak flow event was observed due to the gridded IMD data, sparse station, and the limitations of SRM simulating the rainfall-runoff processes during very heavy rainfall events. Characteristics of the simulated hydrographs and their comparison with the observed hydrographs are shown in Table 4. The subsequent increase is observed in the seasonal measured volume during the years 2011 and 2013, and a slight increase is observed during 2010 and 2012. The computed volume increased during 2010–2013, whereas decreased volume is observed in 2014.
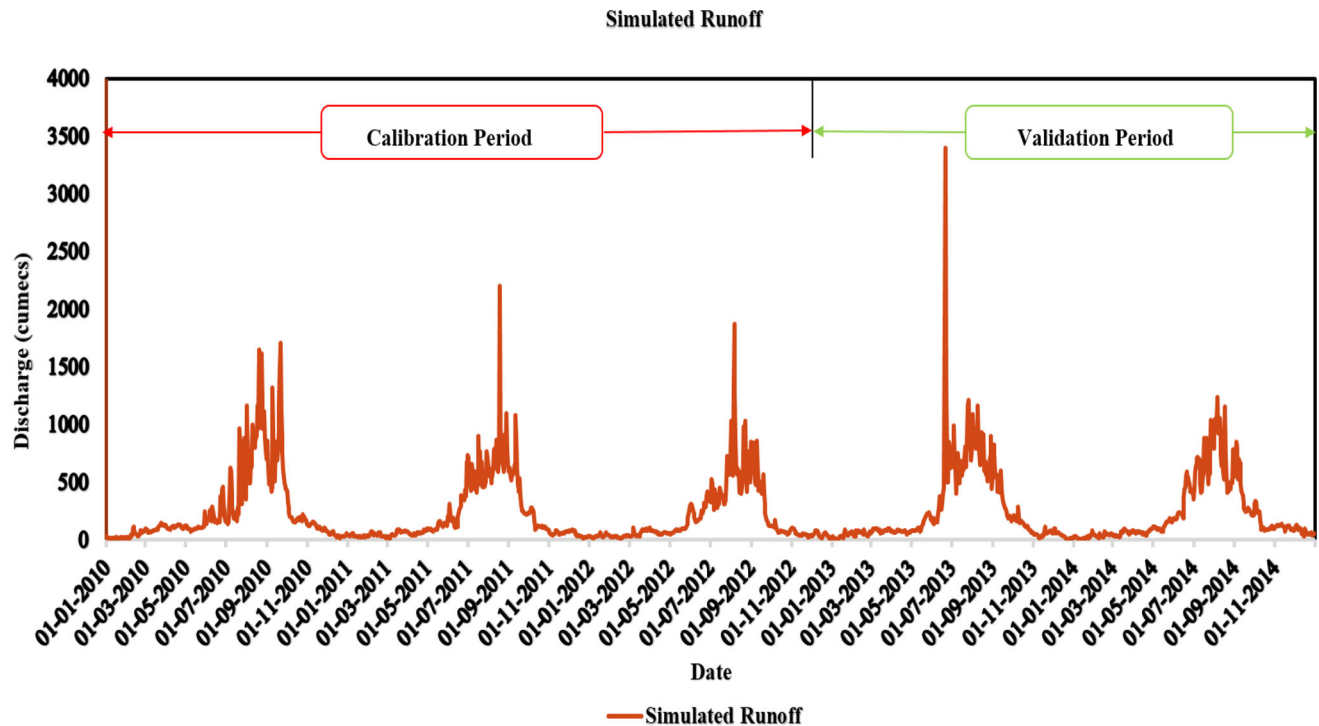
Simulated Runoff

Fig. 8 Simulated runoff hydrograph

Medium discharge rates are estimated for the ablation season (April–May) due to the lowest variability in precipitation (average rainfall 2 cm) and temperature variation. The average measured and simulated runoff rates for 2010 are estimated to be 225.64 and 255.98 m^3/s, respectively. The estimated and simulated discharge rate for the ablation period is found to be in good agreement with each other. During the ablation period, the estimated accuracy range of discharge for all studied hydrological year data is observed to be 0.81 to 0.84 which shows a good correlation between measured and computed runoff. The correlation between the measured and computed discharge range is summarized in Table 4, where the D_v% and R^2 for 2010 to 14 are shown. The simulated daily flow hydrographs for the ablation seasons (April–August) during 2010–2014 are estimated with an average correlation of 0.84. The measured runoff rate is found to be at its lowest value of 25.69 m^3/s in 2013 and a higher rate of 3400.31 m^3/s in 2013. The average discharge rates for the monsoon season (June–August) are estimated to be 519.20, 530.12, 478.69, 689.23, and 585.29 m^3/s during the hydrological years 2010–2014, respectively. Seasonal simulated runoff rate analysis has also been carried out, and the maximum discharge rate of 276.54 m^3/s is observed in 2013 and minimum in 2012 which is about 194.99 m^3/s. It can be inferred that in the Himalayan catchment, the melt runoff which is very important to study can be computed with the openly available remotely sensed datasets. Also, the peak event was captured by the model which is very important as in the case of the Himalayan catchment.

Conclusion and Recommendations

Snowmelt is a vital parameter for models related to climate change, water resources, and studies of glacier health. Studies of snow trend monitoring, snowmelt, and runoff estimation are essential to understand the present scenario and to make climate predictions for future planning and the conservation of natural resources. In this study, snowmelt discharge is estimated for 2010–2014 using satellite-derived inputs and a temperature index approach where hourly datasets are not available, especially for the Himalayan region. Hydro-meteorological datasets (dispersion of precipitation for the period (2010–2014) derived from IMD and SRM hydrographic analysis demonstrate the usage of satellite-based estimations in the modelling. Runoff models calibrated for different study periods and range of discharge (m^3/s) are analysed during the ablation period showing a good correlation between the measured and computed runoff. Satellite-derived SCA is obtained for the period 2010–2014, and variation in the snow cover fraction over the various delineated zones is observed to be high during the winter months and reduced during the summer monsoon season. Further snowmelt is quantified at the glacial surface over the Bhagirathi basin. The model
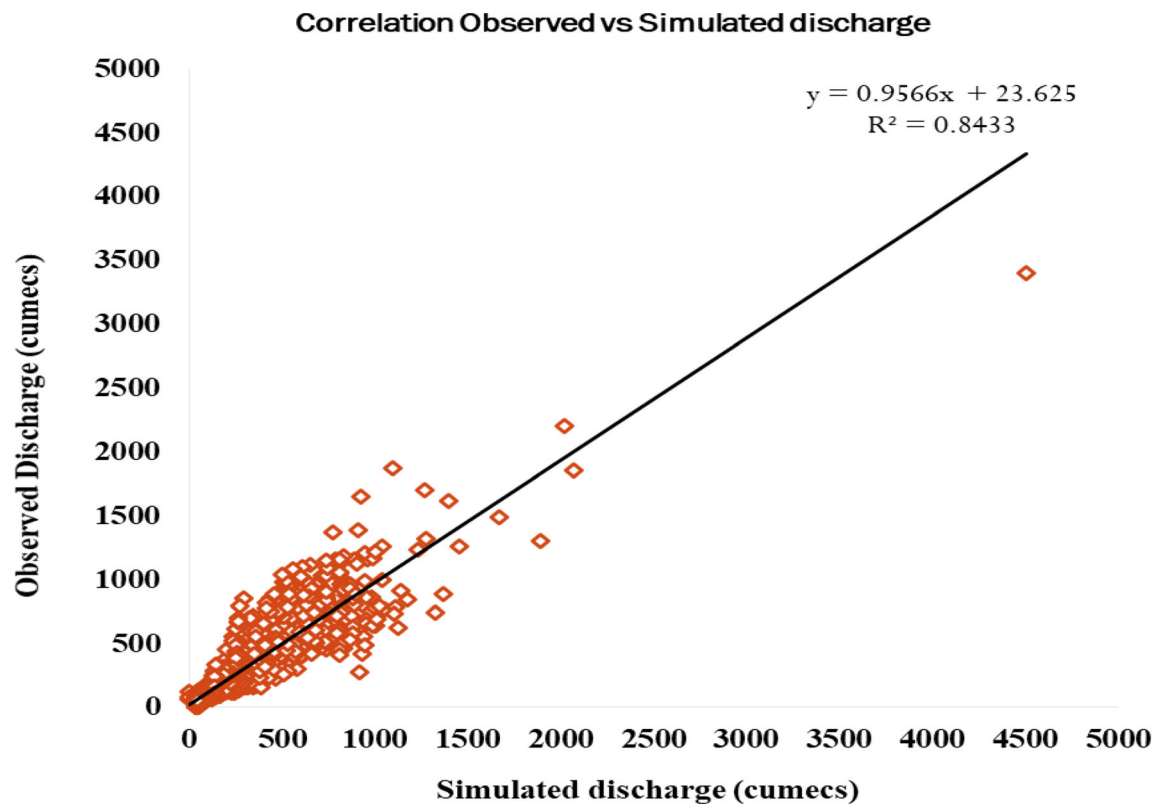
Fig. 9 Correlation of observed and simulated discharge

Table 4 Calibration and validation period

Period considered	R^2	NSE	Volume difference (%)
Calibration period			
2010	0.82	0.71	-10.32
2011	0.81	0.73	3.55
2012	0.815	0.69	4.36
Validation period			
2013	0.82	0.75	7.38
2014	0.84	0.77	-12.45

sensitivity analysis using the SRM parameters, e.g. degree-day factor, runoff coefficient, rainfall coefficient, SCA, and the average daily temperature, shows all these input parameters strongly impacted the model results. The simulated runoff volume for the modelling period is slightly overestimated with a volume difference of $(D_v\%) - 10.32$. The correlation coefficient is found to be high ($R^2 = 0.84$) and NSE = 0.77. The satellite-derived and measured runoff volumes for different time frames are found to be adjoining. Heavy rainfall and high-temperature fluctuations indicate an overestimation of discharge during the monsoon season (June–August). The hydrographs reveal the high snowmelt is most pronounced in the middle elevation areas. Due to the inaccessibility of the complex terrains, the

remotely sensed snow cover is used to complement the estimation of melt runoff using SRM. This is useful for investigations of the present scenario as well as for considering the impacts of climate or increases in temperature leading to glacier melting. The Bhagirathi basin has mostly snow-covered areas, and major tributaries of the river Ganga originating from this zone provide water resources in the foothill regions of India. Therefore, accurate stream-flow simulations are significant for water resource management and planning and provide forecasts of water resource availability. These analyses would help minimize the risks and losses due to floods caused by rapid snow and glacier melt. The improved satellite-derived input parameters have the potential to enhance the accuracy of computations, and hence the runoff prediction capability, particularly in the Himalayan region. The present study can also help estimate the hydropower potential estimation and reservoir operations. The present study may be used as a reference study for the estimation of discharge rates using freely available satellite and meteorological datasets over the western Himalayan region.

Future work may be extended to evaluate the snowmelt runoff of the Ganga River basin with the assimilation of remote sensing-derived basin hydrological parameters such as snow depth and snow water equivalent. Runoff discharge may be evaluated more accurately with the

improved knowledge of the hydro-meteorological variables and land surface parameters such as variations in the glacier area, snowpack parameters, and high-resolution gridded-meteorological input variables. These dynamics may be analysed with advanced space-borne sensors and can be used in discharge simulations for more accurate results. More research should be promoted on the snowmelt runoff modelling feasibility in the mountainous basin where there are limited data available due to the inaccessibility of terrain, by utilizing freely available remote sensing and meteorological datasets. The Bhagirathi basin has a lot of area under glacier cover, the drawback in this model is that it gives total runoff only; it does not partition the melt from glaciers, melt from the snow, and base flow runoff which can be the study for future hydrological modelling in this basin.

Declarations

Conflict of interest None.

References

Abudu, S., Sheng, Z., Cui, C., Saydi, M., Sabzi, H. Z., & King, J. P. (2016). Integration of aspect and slope in snowmelt runoff modeling in a mountain watershed. *Water Science and Engineering, 9*(4), 265–273. https://doi.org/10.1016/j.wse.2016.07.002

Aggarwal, S. P., Thakur, P. K., Nikam, B. R., & Garg, V. (2014). Integrated approach for snowmelt run-off estimation using temperature index model, remote sensing, and GIS. *Current Science, 106*(3), 397–407. https://doi.org/10.18520/cs/v106/i3/397-407

Anderson, E. A. (1973). *National Weather Service River forecast system: Snow accumulation and ablation model* (Vol. 17). US Department of Commerce, National Oceanic and Atmospheric Administration, National Weather Service.

Ångström, A. (1933). On the dependence of ablation on air temperature, radiation and wind. *Geografiska Annaler, 15*(4), 264–295.

Azam, M. F., Wagnon, P., Vincent, C., Ramanathan, A. L., Kumar, N., Srivastava, S., Pottakkal, J. G., & Chevallier, P. (2019). Snow and ice melt contributions in a highly glacierized catchment of Chhota Shigri Glacier (India)over the last five decades. *Journal of Hydrology, 574*, 760–773. https://doi.org/10.1016/j.jhydrol.2019.04.075

Bhambri, R., Bolch, T., Chaujar, R. K., & Kulshreshtha, S. C. (2011). Glacier changes in the Garhwal Himalaya, India, from 1968 to 2006 based on remote sensing. *Journal of Glaciology, 57*(203), 543–556. https://doi.org/10.3189/002214311796905604

Bormann, K. J., Evans, J. P., & McCabe, M. F. (2014). Constraining snowmelt in a temperature-index model using simulated snow densities. *Journal of Hydrology, 517*, 652–667. https://doi.org/10.1016/j.jhydrol.2014.05.073

Bhadra, B. K., Arun, G., Salunkhe, S. S., & Jeyaseelan, A. T. (2015). Snowmelt runoff modelling and its implications in hydropower potential assessment in Dhauliganga catchment of Pithoragarh District, Uttarakhand.

Dobhal, D. P., Gergan, J. T., & Thayyen, R. J. (2008). Mass balance studies of the Dokriani Glacier from 1992 to 2000, Garhwal Himalaya, India. *Bulletin Glacier Research, 25*, 9–17.

Dozier, J. (1989). Spectral signature of alpine snow cover from the Landsat thematic mapper. *Remote Sensing of Environment, 28*(C), 9–22. https://doi.org/10.1016/0034-4257(89)90101-6

Fierz, C., Riber, P., Adams, E. E., Curran, A. R., Föhn, P. M. B., Lehning, M., & Plüss, C. (2003). Evaluation of snow-surface energy balance models in alpine terrain. *Journal of Hydrology, 282*(1–4), 76–94. https://doi.org/10.1016/S0022-1694(03)00255-5

Fily, M., Bourdelles, B., Dedieu, J. P., & Sergent, C. (1997). Comparison of In situ and Landsat thematic mapper derive snow grain characteristics in the Alps. *Remote Sensing of Environment, 59*(3), 452–460. https://doi.org/10.1016/S0034-4257(96)00113-7

Hall, D.K., G.A. Riggs, V.V. Salomonson and G.R. Scharfen, 2001: "Earth Observing System (EOS) Moderate Resolution Imaging Spectroradiometer (MODIS) Snow-Cover Maps," Proceedings of the IAHS Hydrology 2000 Conference, 2–8 April 2000, Santa Fe, NM, pp. 55–60.

Hall, D. K., Riggs, G. A., & Salomonson, V. V. (1995). Development of methods for mapping global snowcover using moderate resolution imaging spectroradiometer data. *Remote Sensing of Environment, 54*, 127–140.

Hock, R. (2003). Temperature index melt modelling in mountain areas. *Journal of Hydrology, 282*(1–4), 104–115. https://doi.org/10.1016/S0022-1694(03)00257-9

Jain, S. K., Goswami, A., & Saraf, A. K. (2010a). Snowmelt runoff modelling in a Himalayan basin with the aid of satellite data. *International Journal of Remote Sensing, 31*(24), 6603–6618. https://doi.org/10.1080/01431160903433893

Jain, S. K., Goswami, A., & Saraf, A. K. (2010b). Assessment of Snowmelt runoff using remote sensing and effect of climate change on runoff. *Water Resources Management, 24*, 1763–1777. https://doi.org/10.1007/s11269-009-9523-1

Joshi, R., Kumar, K., Pandit, J., & Palni, L. M. S. (2015). Variations in the seasonal snow cover area (SCA) for Upper Bhagirathi Basin, India. In R. Joshi, K. Kumar, & L. Palni (Eds.), *Dynamics of climate change and water resources of Northwestern Himalaya. Society of earth scientists series.* Springer. https://doi.org/10.1007/978-3-319-13743-8_2

Kang, D. H. (2005). *Distributed snowmelt modeling with GIS and Casc2d at California Gulch, Colorado* (Doctoral dissertation, Colorado State University).

Khadka, D., Babel, M. S., Shrestha, S., & Tripathi, N. K. (2014). Climate change impact on glacier and snow melt and runoff in Tamakoshi basin in the Hindu Kush Himalayan (HKH) region. *Journal of Hydrology, 511*, 49–60. https://doi.org/10.1016/j.jhydrol.2014.01.005

Kokhanovsky, A. A., Rozanov, V. V., Aoki, T., Odermatt, D., Brockmann, C., Krüger, O., Bouvet, M., Drusch, M., & Hori, M. (2011). Sizing snow grains using backscattered solar light. *International Journal of Remote Sensing, 32*, 6975–7008. https://doi.org/10.1080/01431161.2011.560621

Kulshrestha, S., Ramsankaran, R. A. A. J., Kumar, A., Arora, M., & Senthil Kumar, A. R. (2018). Investigating the performance of snowmelt runoff model using temporally varying near-surface

lapse rate in Western Himalayas. *Current Science, 114*(4), 808–813. https://doi.org/10.18520/cs/v114/i04/808-813

Kult, J., Choi, W., & Choi, J. (2014). Sensitivity of the Snowmelt Runoff Model to snow covered area and temperature inputs. *Applied Geography, 55*, 30–38. https://doi.org/10.1016/j.apgeog.2014.08.011

Kumar, D., Singh, A. K., Taloor, A. K., & Singh, D. S. (2021). Recessional pattern of Thelu and Swetvarn glaciers between 1968 and 2019, Bhagirathi basin, Garhwal Himalaya, India. *Quaternary International, 575–576*, 227–235. https://doi.org/10.1016/j.quaint.2020.05.017

Li, H. Y., & Wang, J. (2008). The snowmelt runoff model applied in the upper Heihe River Basin. *Journal of Glaciology and Geocryology, 30*(5), 769–775.

Li, X. G., & Williams, M. W. (2008). Snowmelt runoff modeling in an arid mountain watershed, Tarim Basin, China. *Hydrological Processes, 22*(19), 3931–3940.

Liu, J. F., Yang, J. P., Chen, R. S., & Yang, Y. (2006). The simulation of snowmelt runoff model in the Dongkemadi River Basin, headwater of the Yangtze River. *Acta Geographica Sinica, 61*(11), 1149–1159.

Liu, W., Li, Z. L., & Li, K. B. (2007). Snowmelt runoff modeling in Tashikuergan River Basin, Xinjiang, China. *Technical Supervision in Water Resources, 3*, 43–46.

Ma, H., & Cheng, G. D. (2003). A test of snowmelt runoff model (SRM) for the Gongnaisi river basin in the Western Tianshan Mountains, China. *Chinese Science Bulletin, 48*(20), 2253–2259.

Mankin, J. S., Viviroli, D., Singh, D., Hoekstra, A. Y., & Diffenbaugh, N. S. (2015). The potential for snow to supply human water demand in the present and future. *Environmental Research Letters*. https://doi.org/10.1088/1748-9326/10/11/114016

Marsh, C. B., Pomeroy, J. W., & Spiteri, R. J. (2012). Implications of mountain shading on calculating energy for snowmelt using unstructured triangular meshes. *Hydrological Processes, 26*(12), 1767–1778. https://doi.org/10.1002/hyp.9329

Martinec, J., & Rango, A. (1986). Parameter values for snowmelt runoff modelling. *Journal of Hydrology, 84*(3–4), 197–219. https://doi.org/10.1016/0022-1694(86)90123-X

Martinec J, Rango A, Roberts R. 1994. Snowmelt runoff model (SRM)user's manual. In *Geographica Bernensia*, Baumgartner MF (ed). Department of Geography, University of Bern: Bern, Switzerland.

Martinec, J. S., Rango, A., & Roberts, R. (2008). *Snowmelt runoff model (SRM), user's manual (updated edition 2008, windows version 1.11)*. USDA Jornada Experimental Range, New Mexico State University.

Narama, A. J., & MacClume, K. L. (2010). *Feasibility report for a Himalayan climate change impact and adaptation assessment*. Centre for International Climate and Environment Research, Oslo and Institute for Social and Environment Transition.

Narama, C., Kääb, A., Duishonakunov, M., & Abdrakhmatov, K. (2010). Spatial variability of recent glacier area changes in the Tien Shan Mountains, Central Asia, using Corona ($\sim$ 1970), Landsat ($\sim$ 2000), and ALOS ($\sim$ 2007) satellite data. *Global and Planetary Change, 71*(1–2), 42–54. https://doi.org/10.1016/j.gloplacha.2009.08.002

Painter, T. H., Dozier, J., Roberts, D. A., Davis, R. E., & Green, R. O. (2003). Retrieval of subpixel snow-covered area and grain size from imaging spectrometer data. *Remote Sensing of Environment, 85*(1), 64–77. https://doi.org/10.1016/S0034-4257(02)00187-6

Pangali Sharma, T. P., Zhang, J., Khanal, N. R., Prodhan, F. A., Paudel, B., Shi, L., & Nepal, N. (2020). Assimilation of snowmelt runoff model (SRM) using satellite remote sensing data in Budhi Gandaki River Basin, Nepal. *Remote Sensing, 12*, 1951. https://doi.org/10.3390/rs12121951

Pai, D. S., Sridhar, L., Rajeevan, M., Sreejith, O. P., Satbhai, N. S., & Mukhopadhyay, B. (2014). Development of a new high spatial resolution (0.25° × 0.25°) long period (1901–2010) daily gridded rainfall data set over India and its comparison with existing data sets over the region. *Mausam, 65*(1), 1–18.

Prasad, V. H., & Roy, P. S. (2005). Estimation of snowmelt runoff in Beas Basin, India. *Geocarto International, 20*(2), 41–47. https://doi.org/10.1080/10106040508542344

Quick, M. C., & Pipes, A. (1995). *UBC watershed model manual*. University of British Columbia. Version 4.0.

Rango, A. (1985). Assessment of remote sensing input to hydrologic models. *Water Resources Bulletin, 21*, 423–432.

RGI Consortium. (2017). *Randolph glacier inventory—A Dataset of global glacier outlines, version 6 [indicate subset used], Boulder, Colorado USA*. NSIDC: National Snow and Ice Data Center. https://doi.org/10.7265/4m1f-gd79

Shrestha, A. B., Agrawal, N. K., Alfthan, B., Bajracharya, S. R., Maréchal, J., & Oort, B. V. (2015). The Himalayan Climate and Water Atlas: Impact of climate change on water resources in five of Asia's major river basins. In: *ICIMOD, GRID-Arendal and CICERO: ICIMOD, GRID-Arendal and CICERO* (pp. 1–96).

Singh, M. K., Thayyen, R. J., & Jain, S. K. (2021). Snow cover change assessment in the upper Bhagirathi basin using an enhanced cloud removal algorithm. *Geocarto International, 36*(20), 2279–2302. https://doi.org/10.1080/10106049.2019.1704069

Singh, S. K., Kulkarni, A. V., & Chaudhary, B. S. (2010). Hyperspectral analysis of snow reflectance to understand the effects of contamination and grain size. *Annals of Glaciology, 51*(54), 83–88. https://doi.org/10.3189/172756410791386535

Sood, V., Gupta, S., Gusain, H. S., Singh, S., & Taloor, A. K. (2021). Topographic controls on subpixel change detection in western Himalayas. *Remote Sensing Applications: Society and Environment, 21*, 100465. https://doi.org/10.1016/j.rsase.2021.100465. ISSN 2352-9385.

Tayal Senzeba, K., Bhadra, A., & Bandyopadhyay, A. (2015). Snowmelt runoff modelling in data scarce Nuranang catchment of eastern Himalayan region. *Remote Sensing Applications: Society and Environment, 1*, 20–35. https://doi.org/10.1016/j.rsase.2015.06.001

Todd Walter, M., Brooks, E. S., McCool, D. K., King, L. G., Molnau, M., & Boll, J. (2005). Process-based snowmelt modeling: Does it require more input data than temperature-index modeling. *Journal of Hydrology, 300*(1–4), 65–75. https://doi.org/10.1016/j.jhydrol.2004.05.002

Thayyen, R. J., & Gergan, J. T. (2010). Role of glaciers in watershed hydrology: A preliminary study of a 'Himalayan catchment.' *The Cryosphere, 4*(1), 115–128.

Tulu, M. D. (2005). *SRTM DEM suitability in runoff studies* (Master of Science thesis, International Institute for Geo-information and Earth Observation, The Netherlands).

Khajuria, V., Kumar, M., Gunasekaran, A., & Rautela, K. S. (2022). Snowmelt runoff estimation Using Combined Terra-Aqua MODIS Improved Snow product in Western Himalayan River Basin via degree day modelling approach. *Environmental Challenges, 8*, 100585. https://doi.org/10.1016/j.envc.2022.100585

Wang, J., Liu, Y., & Li, Y. (2009). Application of SRM to flood forecast and forewarning of Manasi River Basin in Spring. *Remote Sensing Technology and Application, 24*(4), 456–461.

Wulf, H., Bookhagen, B., & Scherler, D. (2016). Differentiating between rain, snow, and glacier contributions to river discharge in the western Himalaya using remote-sensing data and distributed hydrological modeling. *Advances in Water*

Resources, 88, 152–169. https://doi.org/10.1016/j.advwatres.2015.12.004

Zhang, Y. C., Li, B. L., Bao, A. M., Zhou, C. H., Chen, X., & Zhang, X. R. (2006). Simulation of snowmelt runoff model in the Kaidu River Basin. *Science China Earth Sciences, 36*(s2), 24–32.

Zhang, G., Xie, H., Yao, T., Li, H., & Duan, S. (2014). Quantitative water resources assessment of Qinghai Lake basin using Snowmelt Runoff Model (SRM). *Journal of Hydrology, 519*(PA), 976–987. https://doi.org/10.1016/j.jhydrol.2014.08.022